

Measurements and modeling of the admittance matrix at the bridge in guitars

C Lambourg & A Chaigne

Abstract

The 2-D admittance matrix at the bridge of a guitar is derived from measurements of the bridge mobility, both perpendicular and parallel to the top plate. Using high-resolution parametric methods, a mathematical model of this matrix is obtained, where the impulse response for each term is represented by a sum of damped sinusoids. A time-domain modeling of a guitar string is then derived, where string and bridge motions are viewed as vectors with two components. These two components are coupled by means of the cross-terms of the matrix. The numerical model yields realistic simulations of guitar tones. It is shown, in particular, to what extent the tone envelopes are influenced by the coupling at the bridge.

Notations

α	Angle of release
$y(x,t), z(x,t)$	String polarizations
L	String length
A_i	Amplitude
σ_i	Damping factor
φ_i	Phase

F_0	Plucking force
x_0	Plucking position
F_y, F_z	Force at the bridge
V_y, V_z	Bridge velocity
f_i	Frequency
Y_{ij}	Matrix term

1. Introduction

In the standard use of a classical guitar, the finger of the player is directly in contact with the string. Thus, the player can vary a number of plucking parameters (position, force, angle of release) in order to control the quality of the tone (Jansson, 1983). Guitarists know well that altering the angle of release (see Fig. 1) results in strong modifications of the temporal evolution of the sound. Plucking the string perpendicular to the top plate (in the OY direction) usually produces a strong tone which dies out relatively quickly, whereas a parallel pluck (in the OZ direction) produces a softer sound with a longer decay (Richardson, 1988). In order to get a better understanding of these phenomena of great significance for the guitar player, it is necessary to investigate how the vibrational forces from the string are transformed into top plate vibrations through the bridge, since it is the motion of the top plate, and not the motion of the string itself, that creates the sound.

From the point of view of the physicist dealing with stringed instruments, both string and bridge motion can be decomposed into three components: one longitudinal, one perpendicular and one parallel to the top plate. For guitars, experiments show that the longitudinal motion is

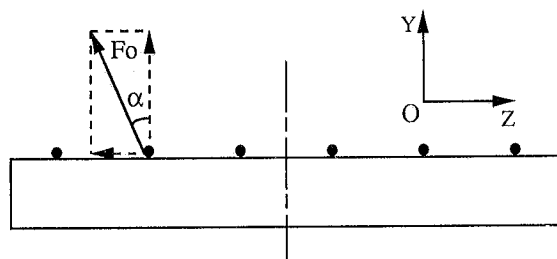


Figure 1: Typical plucking situation in guitar playing

usually smaller than the other two components, and thus this motion will be neglected throughout this work. The relative strength of the y- and z-component depends on the angle of release by the player's finger. The motions of strings and top plate are coupled at the bridge. A measure of the transformation from string force to bridge velocity can be given by the so-called "input admittance" (Moral et al., 1982). Assuming two components for both force and velocity will then lead to the definition of an 2-D admittance matrix at the bridge. The two components are coupled by the cross-terms of the matrix.

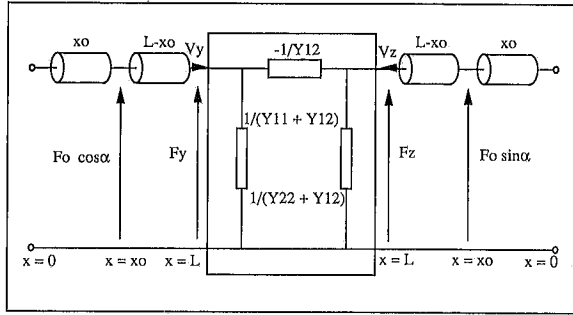


Figure 2: Two string polarizations coupled by an admittance matrix.

In a previous work by the first author, attempts were made to simulate guitar tones using numerical methods in the time domain (Chaigne, 1992). In this latter work, only the vertical motion of string and bridge was considered. One goal here is to improve the existing model by taking the two polarizations of string and bridge into account. Therefore, the first step of the work, presented in Section 3, is to measure the four terms of the admittance matrix at the bridge of a guitar. The purpose of Section 4 is to show how high-resolution parametric methods can be used for modeling the impulse response of each term (Laroche, 1993). With the help of this model, it becomes possible to compute string and bridge waveforms, in order to investigate the influence of the input admittance on the degree of coupling between the two polarizations. Time domain simulations of bridge displacement and velocity are conducted, for different values of the angle of release.

2. Theoretical background

The underlying physical model for the present investigation is shown in Fig. 2. This model is assumed to be linear. The two polarizations of the string are represented by transmission lines of length L . These two polarizations are coupled at one end ($x = L$) by a two-port network, which represents the bridge. The admittance matrix at the bridge is written :

$$\begin{bmatrix} V_y \\ V_z \end{bmatrix} = \begin{bmatrix} Y_{11} & Y_{12} \\ Y_{21} & Y_{22} \end{bmatrix} \begin{bmatrix} F_y \\ F_z \end{bmatrix} \Leftrightarrow [V] = [Y][F] \quad (2.1)$$

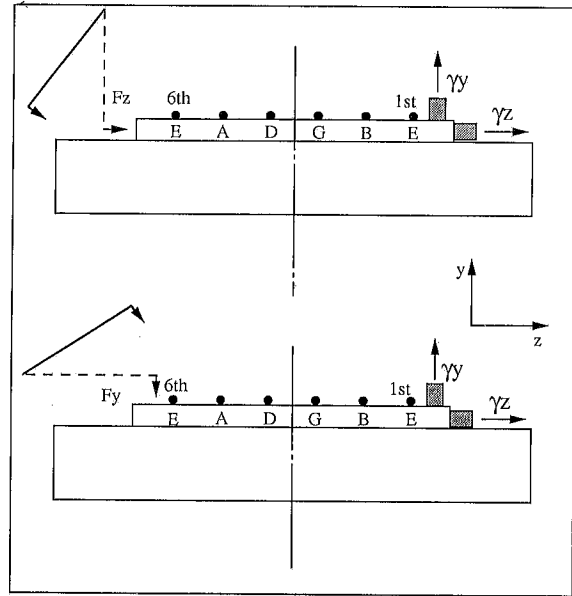


Figure 3: Guitar admittance measurements through impulse excitation.

Due to the reciprocity theorem, in the case of linearity, one has in addition :

$$Y_{12} = Y_{21} \quad (2.2)$$

One can see in Fig. 2, that if the cross-term Y_{12} of the matrix is equal to zero, then the two polarizations are separated. In this case, the temporal evolution of each component only depends on its initial state, and there is no energy exchange between the two components. It is assumed further that the other end of the string (at the neck, or at the fret) is fixed, so that the velocity of both components is equal to zero, for $x = 0$. These boundary conditions are represented by open circuits in Fig. 2. With the help of this model, it becomes possible to compute both components of forces and velocities at any point on the string, once the plucking parameters (F_0 , α , x_0) are given. Our simulation program is based on a time-domain formulation of the transmission lines and of the admittance terms, by means of finite difference methods.

3. Measurements and results

Fig. 3 shows the principles of the experimental set-up. For the sake of clarity, the accelerometers are drawn on the right side of the figure. In practice, acceleration transducers are mounted as close as possible to the point of impact. The force impulse is imparted by a light impact hammer

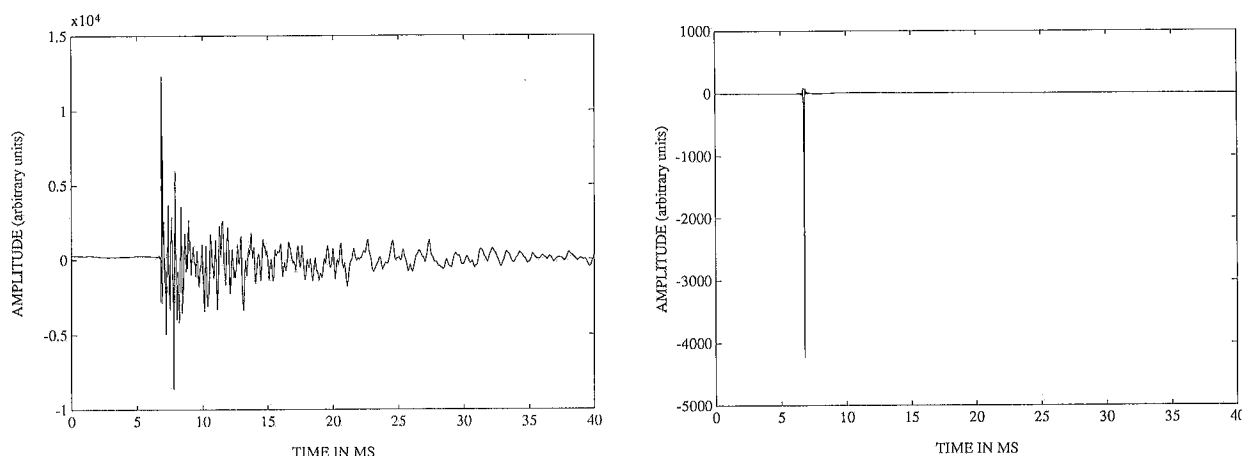


Figure 4: Velocity (left) and force (right) waveforms

B&K 8203 acting as a pendulum. The initial force is measured by a force transducer built in the hammer. Its magnitude depends on the angle of release of the pendulum. The apparatus ensures good reproducibility of the impacts. The velocity signals are obtained through integration of the signals delivered by the accelerometers. Example of waveforms for both velocity and force can be seen in Fig. 4, which represents the first 40 ms of the signals, at a sampling frequency of 48 kHz. Standard FFT procedures applied to these signals yield the admittance term in the frequency domain :

$$Y_{ij}(\omega) = \frac{V_i(\omega)}{F_j(\omega)} \quad (3.1)$$

Fig. 5 shows an example of magnitude frequency response for three terms of the matrix Y_{11} (solid), Y_{12} (dashed), and Y_{22} (dotted), between 0 and 10 kHz. These terms are measured on a medium quality guitar (Picado 1991, N°53). As expected, Y_{11} is the term of highest magnitude, showing that the bridge mobility is more pronounced in the vertical direction than in the horizontal one. The two other terms are of comparable magnitude, at about -20 dB below Y_{11} . However, in some regions, between 0.5 and 1 kHz, and between 2.5 and 4 kHz, for example, all three terms can be of comparable magnitude. As a consequence, the coupling should be more effective in these frequency domains. Other

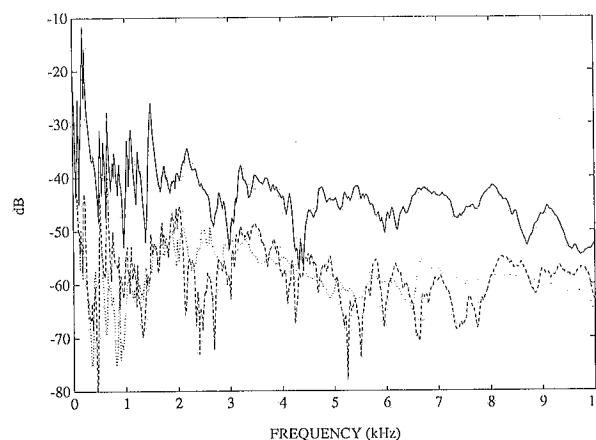


Figure 5: Frequency response for the 3 terms of the admittance matrix.

measurements were performed on a high-quality guitar (Pappalardo 1981, N° 23) showing that both Y_{12} and Y_{22} could be of significantly higher magnitude than Y_{11} for frequencies above 2 kHz.

Several procedures were used, in order to check the reliability of the measurements. Fig 6 shows a comparison between the measured magnitude spectra for Y_{12} and Y_{21} , respectively, which confirms, at least between 0 and 3 kHz, the principle of reciprocity. Other verification procedures involved symmetry properties of the instrument, and the comparison between the results obtained with various exciters and sensors (moving magnet and fixed coil, optical

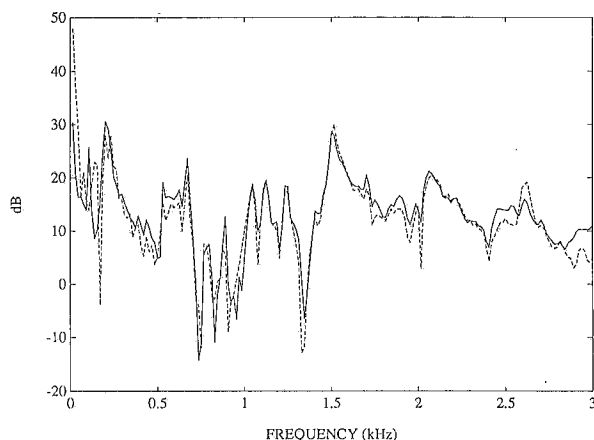


Fig. 6. Verification of the reciprocity theorem. Magnitude spectrum for Y_{12} (solid) and Y_{21} (dashed).

devices,...). Finally, signal processing tools such as time averaging and coherence functions were used, in order to detect a lack in signal-to-noise ratio or the presence of nonlinearities.

4. Modeling the admittance matrix

Once the verification tests made us confident in the obtained results for the admittance matrix, the next step was to find an appropriate model for each term. A time domain high-resolution parametric method (the matrix pencil) was used, which has been proved to be efficient for the modeling of percussive sounds (Laroche, 1993). In this method, the impulse response of a given admittance term (i.e. the inverse Fourier transform of the frequency response) is assumed to be well represented by a sum of damped sinusoids. The

order of magnitude for the number of sinusoids is assumed to be known. In practice, this number can be roughly estimated by a simple preliminary FFT. This basic assumption can be written :

$y(t) = TF^{-1}[Y(\omega)]$ represented by

$$\tilde{y}(t) = \sum_{i=1}^L A_i \exp(-\sigma_i t) \cos(\omega_i t + \phi_i) \quad (4.1)$$

The matrix pencil modeling technique can be summarized as follows. It involves first the diagonalisation of a particular matrix built from the N samples of the signal. From this operation, the complex frequencies (real frequencies f_i and damping factors σ_i) are derived. In a second step, a least-square minimization of the quadratic error between the original signal y and its estimate is performed, which yields amplitudes A_i and phases ϕ_i . (complex residues). Example of the results are shown in Fig. 7, both in the time and frequency domain for Y_{11} . This term is modeled here by a sum of 48 damped sinusoids between 0 and 3 kHz.

No differences can be visually detected between measured and simulated impulse response in Fig.7. With 48 sinusoids, the quadratic reconstruction error is -30 dB below the rms value of the original signal. Useful experiments can be carried out, at this stage, by extracting the most energetic sinusoids from the model.

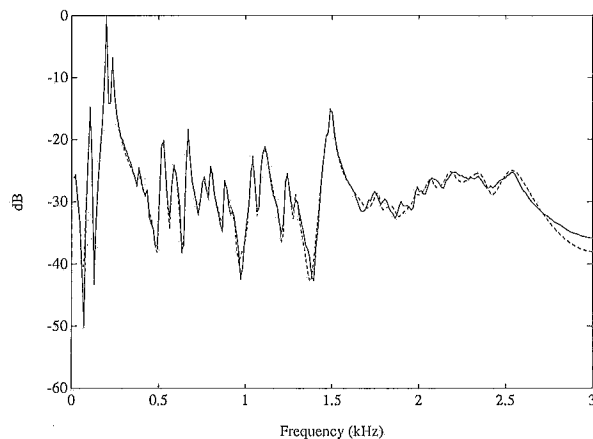
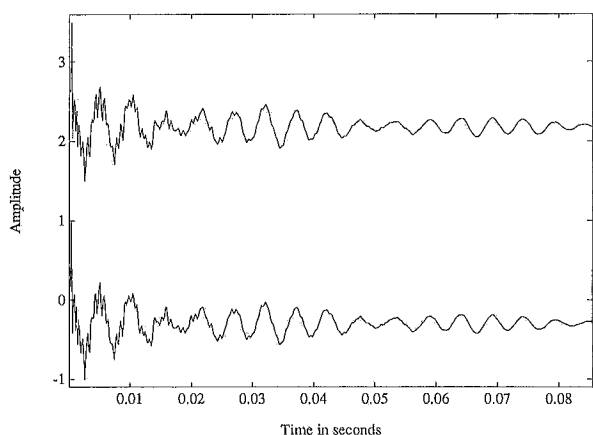


Figure 7: Modeling of admittance term Y_{11} . Left: measured (top) and simulated (bottom) impulse response; Right: measured (solid) and simulated (dashed) frequency response.

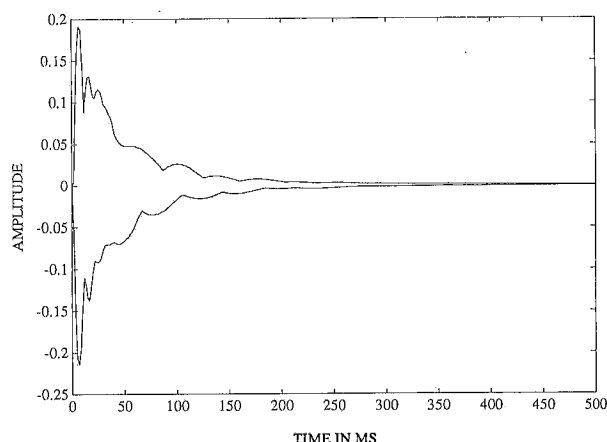


Fig. 8-a). Bridge Velocity V_y ; $\alpha = 0^\circ$

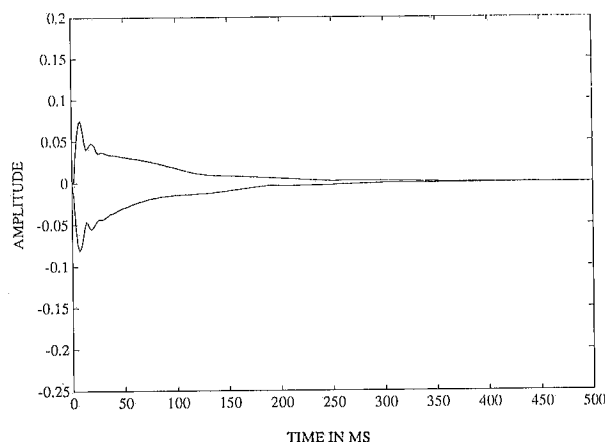


Fig. 8-b). Bridge Velocity V_z ; $\alpha = 90^\circ$

Reconstructing the signal, for example, using only the 15 most energetic components among 48, leads to a quadratic error nearly -15 dB below the rms value. Interesting tones can be simulated, by taking more and more components into account (Sound Example) giving insight into the perceptual significance of the bridge mobility. Fig. 7 shows further a comparison between measured and simulated frequency response for Y_{II} . The number of sinusoids here is still equal to 48. Slight discrepancies less than or nearly equal to 2 dB can be seen locally in the magnitude spectrum, especially for frequencies above 1 kHz.

5. Time-domain synthesis

The modeling part of the work presented in Section 4 can be seen as a modal analysis in the time domain. The last step before time-domain synthesis now consists in deriving a mechanical filter from the modal data, whose impulse response can be represented by a sum of damped sinusoids. One straightforward method is to adopt a parallel representation for the filter, where the impulse response for each branch corresponds to one damped sinusoid of the model. It becomes then tempting to model each branch of the filter by a resonant circuit, consisting of a mechanical resistance, a modal mass and a modal stiffness in series. However, one has to bear in mind that forcing the values of the phases is a necessary condition for this simple representation. This point has already been discussed by other authors, within the context of modal analysis of musical instruments in the frequency domain (Marshall, 1985).

Two examples of bridge velocity waveforms

are shown in Fig. 8. Fig. 8-a) shows the temporal envelope of the vertical component, for a guitar D-string initially plucked perpendicular to the top plate. This envelope exhibits a complicated pattern resulting from the superposition of multiple beats, a consequence of the interaction between string partials and bridge resonances. Fig. 8-b) shows the temporal envelope of the horizontal component, for the same string initially plucked parallel to the top plate (i.e. with a angle of release $\alpha = 90^\circ$) with the same force. As expected, the initial amplitude is smaller in this case than for the perpendicular pluck, since the mobility of the instrument is usually small in this direction. This figure shows less beats and a smoother envelope than for the vertical pluck. In addition, a discontinuity in the slope is clearly seen on this envelope, after about 150 ms. This characteristic feature is a direct consequence of the coupling between the two components due to the presence of cross-terms in the admittance matrix.

Another interesting consequence of the coupling between the two polarizations is displayed in Fig. 9. This figure shows Y-Z plots of bridge displacement, for an initial perpendicular and an initial parallel plot, respectively. Without the presence of coupling terms in the admittance matrix, these plots should be straight lines, in the OY- or OZ-direction, respectively. Here, a precession can be clearly seen in both cases. Notice that the angle of the precession axis is not equal to the angle of release.

6. Conclusion

A time domain modeling of guitar strings has been

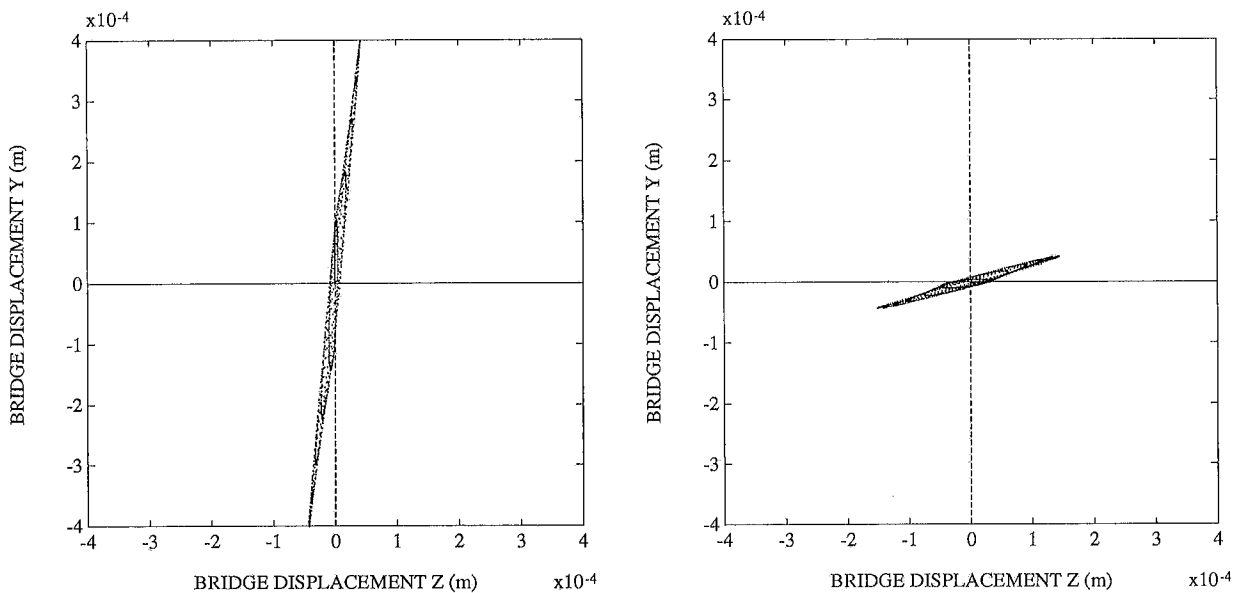


Figure 9: Y-Z plots of bridge displacement. (Left) Initial pluck perpendicular to the top plate; (Right) Initial pluck parallel to the top plate.

developed, where the string is loaded by an admittance matrix at the bridge. The results highlight the fact that the bridge admittance of the instrument has an influence on the temporal evolution of the tones, as it has been already shown theoretically in previous works devoted to other families of string instruments (Weinreich, 1977). However, this effect is limited to the frequency range where all terms of the admittance matrix are of comparable magnitude, as it is usually the case for medium quality guitars.

Acknowledgments

Preliminary experiments on guitars reported in this paper were conducted at KTH Stockholm, during Fall 1990, as the second author was a guest researcher at the Department of Speech Communication and Music Acoustics. The authors would like to thank Erik Jansson for his help in measuring the input admittances, and for many valuable discussions on this subject.

References

- Chaigne A. (1992), "On the use of finite differences for musical synthesis. Application to plucked stringed instruments", *J. Acoustique* 5(2), 181-211.
- Jansson, E. (1983), "Acoustics for the guitar player", in (E. Jansson, ed.) *Function, Construction and Quality of the Guitar*, Stockholm : Royal Swedish Academy of Music, No 38, 7-26.
- Laroche J. (1993), "The use of the matrix pencil method for the spectrum analysis of musical signals", *J. Acoust. Soc. Am.* 94 (4), pp.1958-1965.
- Marshall K. D. (1985), "Modal analysis of a violin", *J. Acoust. Soc. Am.* 77(2), pp. 695-709.
- Moral J.A. & Jansson E.V.(1982), "Eigenmodes, input admittances, and the function of the violin", *Acustica* 50(5), pp. 329-337.
- Richardson B. E. (1988), "Vibrations of stringed musical instruments", University of Wales review, No 4, pp. 13-20.
- Weinreich G. (1977), "Coupled piano strings", *J. Acoust. Soc. Am.* 62(6), pp. 1474-1484.